Capture of Small Paramagnetic Particles by Magnetic Forces from Low Speed Fluid Flows

DANIEL L. CUMMINGS
DAVID A. HIMMELBLAU
JOHN A. OBERTEUFFER
and
GARY J. POWERS

Department of Chemical Engineering
Carnegie-Mellon University
Pittsburgh, Pennsylvania 15213

High gradient magnetic separators are able to capture small, dilute, paramagnetic particles from high velocity fluid flows. Capture cross sections are computed and correlated with dimensionless groups for a bare ferromagnetic collector.

SCOPE

Differences in magnetic properties long have been considered as a possible means for separating mixtures. Magnetite is separated from silaceous rock by large magnetic drum separators. Many processes are protected from damage due to broken gears and other such pieces of magnetic metal by magnetic separators. In these cases, the particles are ferromagnetic, and the separation is relatively easy. However, the separation of very weakly magnetic or paramagnetic particles requires a more sophisticated separator design. One means for carrying out a magnetic separation is to place small diameter (100 μ) ferromagnetic filaments in a solenoid magnetic through which a fluid containing paramagnetic particles is passing. Field gradients are formed in the region surrounding the filaments so that the paramagnetic particles are attracted to and held on the filament. In a practical separator, 2 to 15 vol. % of the magnetic field is filled with filamentary ferromagnetic material. A fluid containing the paramagnetic particles is passed through the matrix formed by the filaments. The paramagnetic material is retained in the matrix while the nonmagnetic particles and fluid pass through. The performance of these separators depends on how efficiently they capture small paramagnetic particles and how much of this material can be retained in the matrix. In this paper we present a theoretical study of the capture efficiency of a single filament of ferromagnetic material. The goal is to develop an understanding of the capture mechanisms involved. The model assumes a single bare filament, a low concentration of particles, and a fluid moving at low speeds. The equations for the magnetic, drag, and gravitational forces acting on a particle are derived and solved for a number of different conditions. The efficiency of the collector is analyzed in terms of its capture cross section.

CONCLUSIONS AND SIGNIFICANCE

This paper presents a detailed analysis of the equations which describe the inertial, magnetic, fluid, and gravitational forces that govern the motion of a small paramagnetic particle near a bare cylindrical, ferromagnetic filament. These equations may be solved numerically to show that particle capture occurs primarily on the front of the cylinder when the flow field is parallel to the magnetic field and perpendicular to the filament. However, in several cases the particles are captured on the downstream side of the collector. A set of seven dimensionless groups can be used to describe the system. The group $N_M = \mu_f H_o^2/\rho_f v_\infty^2$ is defined to express the magnetic field strength.

The magnetic force is long range and is the dominant factor in particle capture. The magnetic force acting on a paramagnetic particle in the vicinity of a ferromagnetic collector can be 100 times greater than gravity. The capture cross section of a bare collector in a magnetic field can be 100 times larger than that due to inertial impaction alone. Many materials which are not commonly thought of as being magnetic (copper oxide, aluminum) can be captured in this type of separator.

Magnetic separation has been used for several centuries to remove magnetic solids from nonmagnetic solids and from fluids. The separation of magnetic minerals from ores has been the largest commercial application. Over 100,000 tons of iron ores were processed by magnetic means in 1973. The magnetic separator industry has sales of over ten million dollars per year. Experience in the design of magnetic separators for ore processing has produced separators that are both efficient and mechanically reliable (Lawver, 1974).

The chemical process industries have not used magnetic separators to any great extent. The most widely used magnetic separators in chemical processes are small permanent magnet separators which protect mechanical equipment such as grinders and pumps from stray pieces of metal such as broken gear teeth and nuts and bolts. Most

Correspondence concerning this paper should be addressed to Gary J. Powers. Daniel L. Cummings is with the Aluminum Company of America, Technical Center, Alcoa Center, Pennsylvania 15069. David A. Himmelblau is with Energy Resources, Inc., Cambridge, Massachusetts 02141. John A. Oberteuffer is with Sala Magnetics, Cambridge, Massachusetts 02142.

attempts to apply magnetic separation to more complex solid-solid and solid-liquid separation problems have been failures. The particles are ordinarily not as magnetic as magnetite (Fe_3O_4), the primary iron ore separated by magnetic means. Hence the magnet force acting on the particles was not large enough to effect the separation.

Over the last 5 yr a number of applications of modern magnet design has given rise to magnetic separators which have the potential for use in the chemical process industries (Kolm et al., 1975). These separators can generate magnetic forces from 1 to 3 orders of magnitude greater than those available with the previous separator design (Oberteuffer, 1974). They do this by creating large fields and large field gradients about a collector. These separators commonly involve a solenoid electromagnet which has its interior filled with a ferromagnetic matrix. This matrix usually takes the form of either thin, randomly packed metal strands or metal screens. The mixture to be separated is passed through the matrix when the solenoid is energized. The paramagnetic particles are captured and held on the matrix, while the nonmagnetic materials pass through. When the matrix is loaded with captured particles, the magnetic field is removed by deenergizing the solenoid. The paramagnetic material may then be flushed out of the matrix and the cycle repeated. A number of continuous separators have been designed which move the matrix through the field region where it is loaded (Lawver, 1974). This new type of separator design generates sufficient force to affect materials such as copper oxide and aluminum which are not ordinarily considered magnetic.

Several commercial applications of this concept have been successful. The largest one is in the kaolin clay industry where very weakly magnetic titanium dioxide and iron stained kaolin particles are removed from raw clay. The result is a white clay which has a high market value. The magnetic separation process is more economical than froth flotation and chemical leaching for this process. Several of the separators used in this industry are very large. One unit has an internal diameter of 2 m, weighs 250 tons, and processes 60 tons of clay/hr. Other potential applications under current study are the desulfurization of coal (Trindade et al., 1974), the removal of ash from liquid coal, the treatment of wastewater (DeLatour, 1973), and the beneficiation of semitaconite iron ores (Kelland, 1973, 1974; Lawver, 1974). The technique appears useful for a wide range of particulate systems. If the particles are weakly magnetic, they may be removed directly. If they are not magnetic, magnetic seeding may be used so that magnetic separation can be effected (Mamula, 1969).

The performance of a magnetic separator depends on the ability of the matrix to selectively capture and hold the particles. Watson (1973, 1975) and Bean (1971) have developed mathematical models for magnetic separators. These models require knowledge of how particles are captured on magnetic collectors. In this paper we develop the equations for the capture of small paramagnetic particles on bare collectors from low-speed flows. The loading of a collector will be discussed in a following paper. The matrix is represented by a single infinite ferromagnetic cylinder immersed in a uniform magnetic field. A Newtonian fluid flows across the cylinder and parallel to the magnetic field. Paramagnetic particles enter upstream from the collector and, depending on the conditions of the system, may be captured.

In the following sections, the basic electromagnetic and fluid flow equations are developed for this system. The equations are solved numerically, and particle trajectories are presented for several interesting cases. The capture cross section is shown to depend on a small number of dimensionless groups which can be derived from the basic equations.

FORCES ACTING ON A PARTICLE IN A MAGNETIC SEPARATOR

Consider a small particle near a ferromagnetic cylinder which is in a magnetic field. The path of the particle is dependent on the gravitational, inertial, drag, and magnetic forces acting on it. In the following sections, the equations for each of these forces are presented. The equation for the sum of the forces is then solved numerically to give the trajectory of the particle in the region surrounding the collector.

THE FORCE ON A SPHERICAL BODY IN A NONHOMOGENEOUS MAGNETIC FIELD

The magnetic field in a region surrounding a ferromagnetic collector which has been placed in a uniform magnetic field is distorted by the field generated in the collector. The field is higher in certain regions near the surface of the collector. A paramagnetic particle near the collector is attracted to the higher field region. In this section the equations for the magnetic fields and forces are presented. The key assumptions required in the derivations are discussed.

Consider a small spherical paramagnetic particle in a uniform magnetic field. The magnetic permeability of the region is μ_f and of the particle is μ_p. The energy change which results from the introduction of the particle is

$$W' - W = -\frac{1}{2}\int_{V_p} (\mu_p - \mu_f)\,\mathbf{H}\bullet\mathbf{H}'\,dV_p \qquad (1)$$

In order to use Equation (1), it is necessary to know the field $\mathbf{H}$ inside the particle after it has been introduced into the field region. For a sphere with its polar axis (z direction) coincident with the direction of the uniform field $\mathbf{H}_o$ and with polar angle θ

$$\mathbf{H}' = \frac{3\mu_f}{\mu_p + 2\mu_f} H_o(\mathbf{i}_r \cos\theta - \mathbf{i}_\theta \sin\theta) \qquad (2)$$

Combining Equation (2) with (1) and integrating, we get

$$W' - W = -\frac{1}{2}\frac{\mu_f(\mu_p - \mu_f)}{\mu_p + 2\mu_f} H_o^2\, 4\pi R_p^3 \qquad (3)$$

If there exists a small irregularity $\Delta H << H_o$ in the otherwise uniform magnetic field (that is, a disturbance in the uniform field caused by the ferromagnetic collector), a force will act on the sphere. The force is obtained by considering the work required to move the sphere a distance Δx. The magnetic force is given by

$$\mathbf{F}_M = \frac{\mu_f(\mu_p - \mu_f)}{\mu_p + 2\mu_f} 2\pi R_p^3\, \nabla(\mathbf{H}\bullet\mathbf{H}) \qquad (4)$$

In order to determine the force on the particle, it is necessary to know the gradient in the magnetic field surrounding the collector. Consider the infinite cylinder (collector) in Figure 1. The cylinder is made of a ferromagnetic material and is immersed in a uniform magnetic field. Stratton (1941) has derived the following equations for this case. The field surrounding the cylinder is given by

$$\mathbf{H} = [H_o(\mathbf{i}_r \cos\theta - \mathbf{i}_\theta \sin\theta)] + H_o\left(\frac{R_c}{r}\right)^2\left(\frac{\mu_c - \mu_f}{\mu_c + \mu_f}\right)[\mathbf{i}_r \cos\theta + \mathbf{i}_\theta \sin(\theta)] \qquad (5)$$

The first term is due to the applied field and the second term is due to the magnetization of the cylinder.

Combining Equations (4) and (5), we get

$$\mathbf{F}_M = -(8\pi R_p^3 R_c^2 H_o \alpha)\left(\frac{\mu_p \gamma}{\gamma+3}\right)\left[\mathbf{i}_r\left(\frac{\alpha R_c^2}{r^5}+\frac{\cos 2\theta}{r^3}\right)+\mathbf{i}_\theta\left(\frac{\sin 2\theta}{r^3}\right)\right] \quad (6)$$

where

$$\alpha = (\mu_c - \mu_f)/(\mu_c + \mu_f) \quad (7)$$

$$\gamma = (\mu_p/\mu_f) - 1 \quad (8)$$

Typical magnetic force contours are given in Figure 2. Note that a repulsive force region exists along the y axis. This figure is similar to the one developed by Zebel (1965) for electric fields. Experimental confirmation of these repulsive regions has been made by Himmelblau (1974).

DRAG FORCES

The drag force acting on a spherical particle is given by

$$\mathbf{F}_D = 6\pi\eta R_p \mathbf{v}_{pr} \quad (9)$$

where $\mathbf{v}_{pr}$ is the particle velocity relative to the fluid

$$\mathbf{v}_{pr} = \mathbf{v}_f - \mathbf{v}_p \quad (10)$$

The use of Equation (9) implies that the flow around the particle is in the Stokes' regime. This is true as long as $\mathbf{v}_{pr}$ is small, which is the case for small particles that essentially follow the fluid streamline. The use of Equation (9) to compute the drag force requires the fluid velocity in the region surrounding the collector.

Consider an incompressible fluid of constant viscosity η in steady potential flow around the collector. For potential flow

$$\rho \mathbf{v} \cdot \nabla \mathbf{v} = -\nabla \rho \quad (11)$$

For the assumption that

$$\nabla \times \mathbf{v} = 0 \quad (12)$$

the solution to Equations (29) and (30) is

$$\mathbf{v}_f = \mathbf{i}_r v_\infty \cos\theta\,[1-(R_c^2/r^2)] - \mathbf{i}_\theta v_\infty \sin\theta\,[1+(R_c^2/r^2)] \quad (13)$$

Equations (9) and (13) can then be combined to determine the drag force acting on a particle in the region surrounding a collector.

GRAVITATIONAL FORCE

The net gravitational force acting on a particle immersed in a fluid is given by

$$\mathbf{F}_g = (\rho_p - \rho_f)\frac{4}{3}\pi R_p^3 g(\mathbf{i}_r \cos\theta - \mathbf{i}_\theta \sin\theta) \quad (14)$$

For the situation shown in Figure 1, $\mathbf{F}_g$ is entirely in the $\mathbf{i}_x$ direction.

FORCE BALANCE

The net force acting on a particle is

$$\mathbf{F}_p = \frac{4}{3}\pi R_p^3 \rho_p \frac{d\mathbf{v}_p}{dt} = \mathbf{F}_M + \mathbf{F}_D + \mathbf{F}_g \quad (15)$$

In dealing with small particles ($< 10 \times 10^{-6}$m), the mass of the particle is small enough that inertia may usually be neglected, and the force balance becomes

$$0 = \mathbf{F}_M + \mathbf{F}_D + \mathbf{F}_g \quad (16)$$

Both forms are considered in this analysis. Equation (15) may be written in dimensionless form as

$$\left(\frac{Re_p}{9}\right)\frac{dv_p'}{d\tau} = \left(\frac{-2R_c'}{3}\right) Re_c N_M \alpha \Gamma \left[\mathbf{i}_r\left(\frac{\alpha R_c'^2}{r'^5}+\frac{\cos 2\theta}{r'^3}\right)+\mathbf{i}_\theta\left(\frac{\sin 2\theta}{r'^3}\right)\right] + (\mathbf{v}_p' - \mathbf{v}_f') + N_g(\mathbf{i}_r \cos\theta - \mathbf{i}_\theta \sin\theta) \quad (17)$$

where

$$\alpha = \left(\frac{\mu_c - \mu_f}{\mu_c + \mu_f}\right) \quad (18)$$

$$\Gamma = \left(\frac{\gamma}{\gamma+3}\right), \quad \gamma = \left(\frac{\mu_p}{\mu_f} - 1\right) \quad (19)$$

$$N_M = \left(\frac{\mu_f H_o^2}{\rho_f v_\infty^2}\right) \quad (20)$$

$$R_c' = (R_c/R_p) \quad (21)$$

$$Re_p = \left(\frac{\rho_p v_\infty 2R_p}{\eta}\right) \quad (22)$$

$$Re_c = \left(\frac{\rho_f v_\infty 2R_c}{\eta}\right) \quad (23)$$

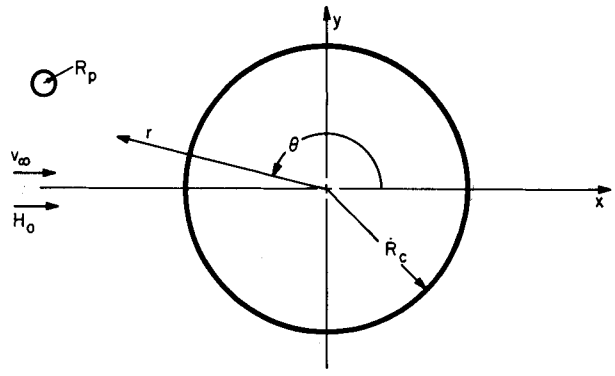

Fig. 1. System geometry for capture of a small paramagnetic particle on a ferromagnetic wire. The particle size R_p is much less than R_c.

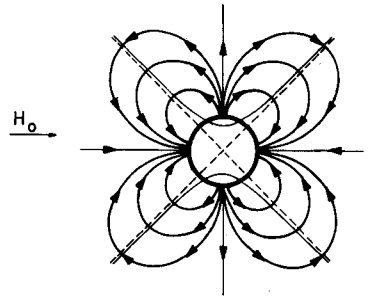

Fig. 2. Magnetic force contours for an infinite ferromagnetic cylinder immersed in a uniform magnetic field. The contours indicate the forces which act on a small paramagnetic particle in the region surrounding the cylinder. Note the repulsion regions perpendicular to the applied field. The hyperbolae indicate the lines of zero radial force.

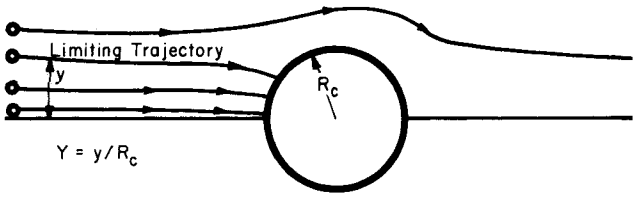

Fig. 3. Capture cross section Y for small paramagnetic particles being captured by a ferromagnetic cylinder.

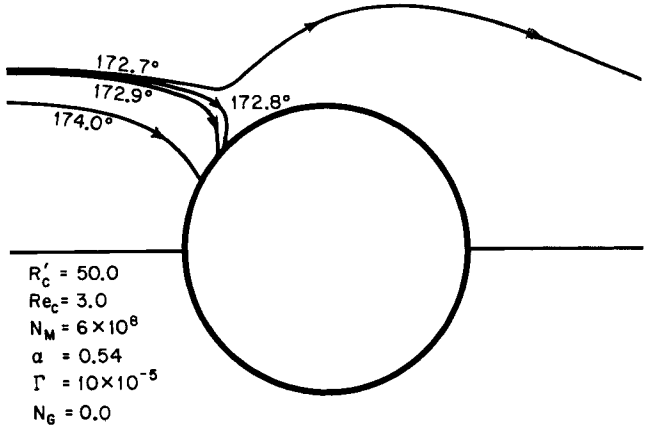

Fig. 5. Particle trajectories with an applied magnetic field. Note the effects of the repulsive magnetic force region.

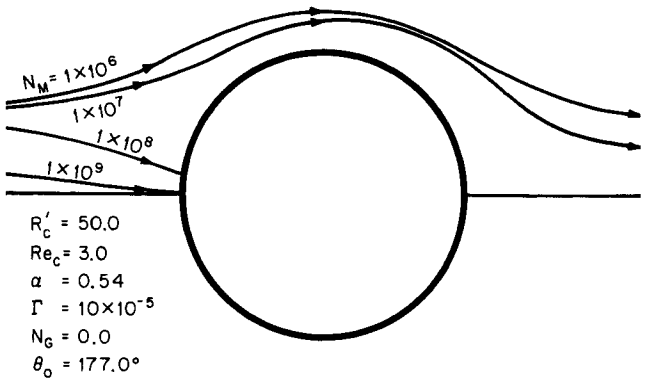

Fig. 7. Effect of magnetic field strength on particle trajectories. All particles started at the same location.

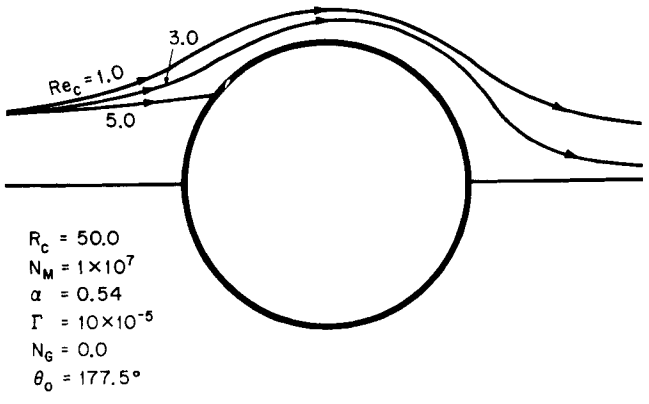

Fig. 8. Effect of Reynolds' number on particle trajectories. All particles started at the same location.

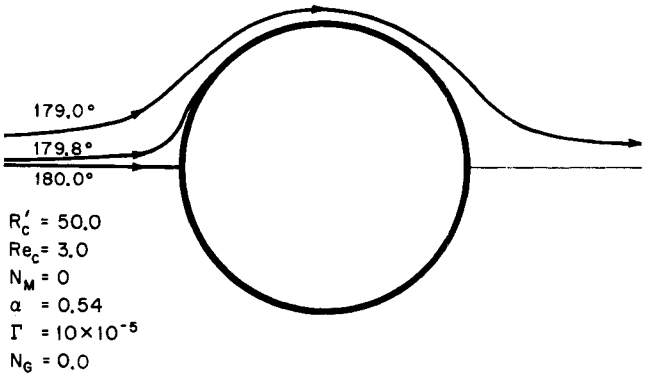

Fig. 4. Particle trajectories with no magnetic field. The capture mechanism is inertial impaction or direct interception.

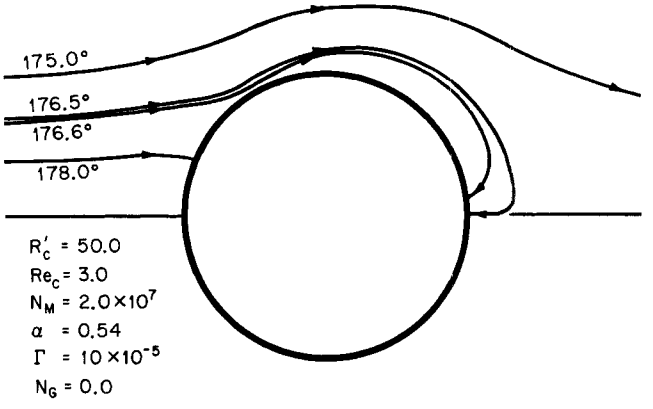

Fig. 6. Back side capture.

$$N_g = \left[\frac{2R_p^2(\rho_p - \rho_f)g}{9\eta v_\infty}\right] \tag{24}$$

$$r' = (r/R_p) \tag{25}$$

$$v_f' = (v_f/v_\infty) \tag{26}$$

$$v_p' = (v_p/v_\infty) \tag{27}$$

$$\tau = (t\, v_\infty/R_p) \tag{28}$$

Setting the left-hand side of Equation (17) equal to zero (small particle case), we get the dimensionless form for Equation (16).

PARTICLE TRAJECTORIES

Equations (15) and (16) were solved numerically for a number of different particle, collector, and fluid conditions. The objective was to determine both the individual particle capture characteristics as well as the capture cross section Y, defined in Figure 3.

Equation (15) was solved by a fourth-order Runge-Kutta technique, solving for v_p and then computing

$$\Delta r = \Delta t\,(v_p \bullet i_r) \tag{29}$$

$$\Delta\theta = \Delta t\,[(v_p/r) \bullet i_\theta] \tag{30}$$

Equation (16) (no inertia) may be used to solve for v_p algebraically. With appropriate restrictions on Δr and $\Delta\theta$, Y, computed algebraically, agrees with Y computed by the Runge-Kutta method to within 5% while computation time is reduced by 2 orders of magnitude. The necessary restrictions were found to be

$$\Delta r \leq R_p \tag{31}$$

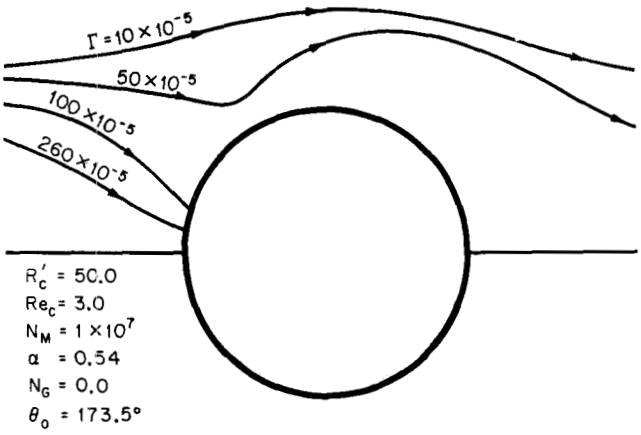

Fig. 9. Effect of particle permeability on particle trajectories. All particles started at the same location.

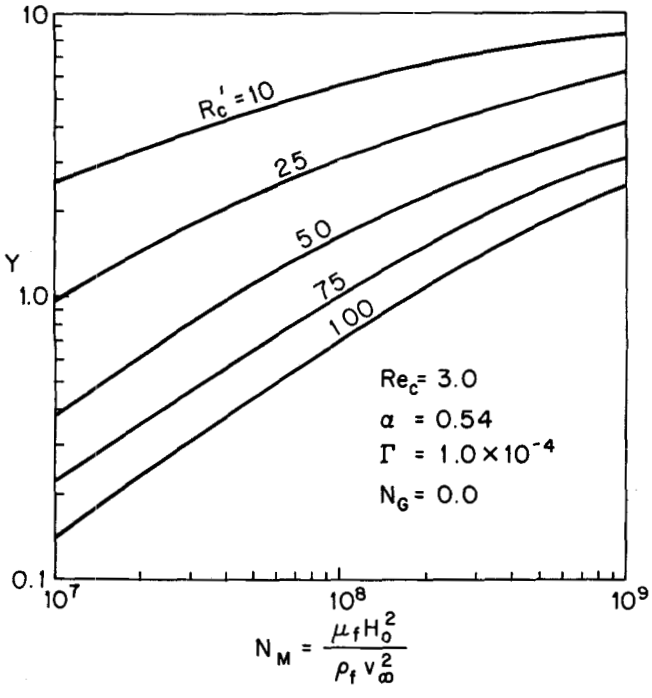

Fig. 11. Effect of particle size on capture cross section.

$$\Delta\theta \leq 1^{\circ} \qquad (32)$$

Several different classes of trajectories are shown in Figures 4, 5, 6, 7, 8, and 9. While most of the particles are captured on the front of the collector, some can be trapped on the back. Back capture is rare, since a repulsive magnetic force region exists near the $\theta = \pi/2$ sector of the collector. These calculations are reinforced by the experiments of Himmelblau in which photographs were taken of the captured particles (Himmelblau, 1974). Himmelblau found front side capture to predominate and observed only occasional back side collection. These studies were confined to laminar flow around the collector. Himmelblau observed more back side capture when the flow rate was high enough to cause a turbulent wake behind the collector. The amount of back side capture was still small, however. Capture was assumed to occur when the particles' surface touched the surface of the collector. Himmelblau did observe some movement of particles after they became attached to the surface of the collector. No bouncing after impact was observed during his experiments.

All particles were assumed to start from rest at 10 collector radii upstream from the collector. The starting angle at this radius is given on the figures.

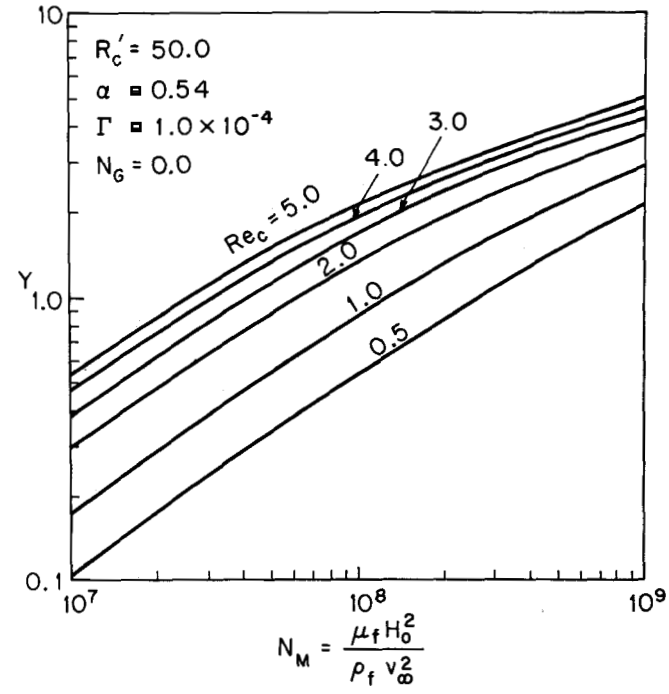

Fig. 10. Effect of Reynolds number on capture cross section.

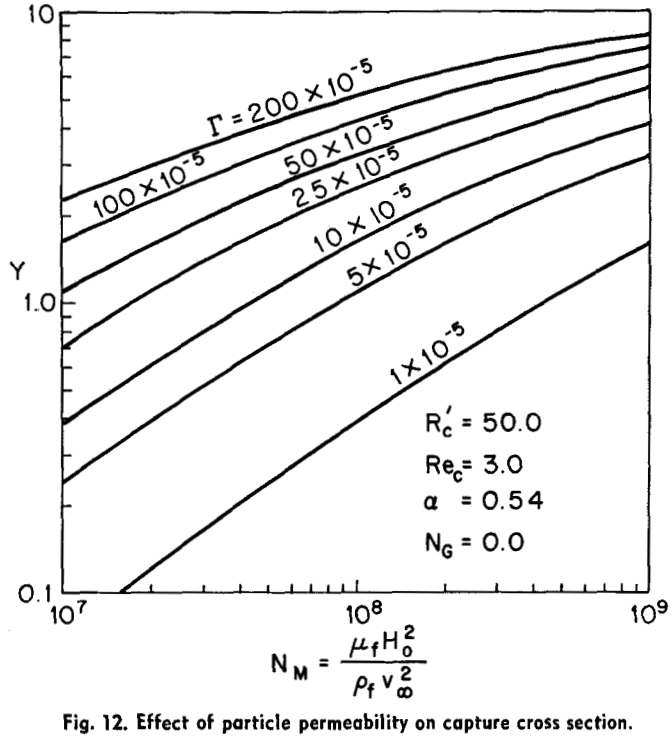

Fig. 12. Effect of particle permeability on capture cross section.

COMPUTED CAPTURE CROSS SECTIONS

The capture cross section of a bare cylindrical collector was determined under a wide range of conditions. The calculations were first done by assuming that all of the dimensionless groups were independent. The dependence of the cross section on the key dimensionless groups is shown in Figures 10, 11, and 12.

A second calculation was performed from the point of view of the laboratory experiments. It was assumed that the carrier fluid and collector material are fixed and that the flow rate, particle permeability, and magnetic field are the variables. Selection of water as the fluid fixes ρ_f, η, and μ_f. Selection of annealed iron as the collector material fixes $\mu_o M_c$ ($= 2.16$ w/m^2) and thereby makes α a function of the applied field. If the fluid and collector

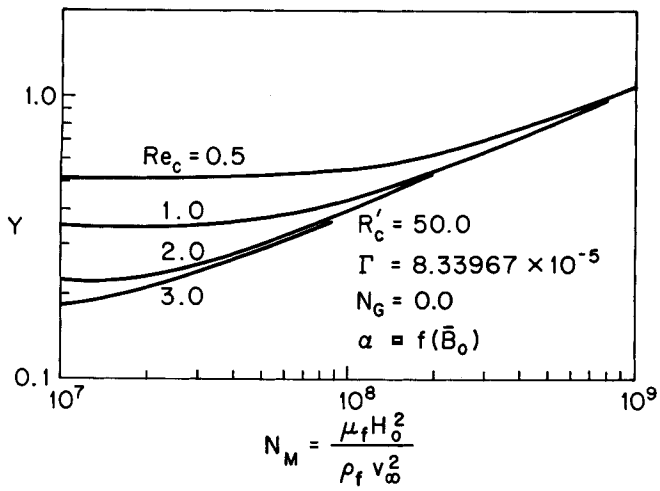

Fig. 13. Effect of Reynolds number on capture cross section. The fluid is water, the collector is annealed iron, and the particle is copper oxide. Fixing the fluid, collector material, and R_c' means that Re_c and N_M are related through v_∞. The functioon $\alpha = f(B_0) = \mu_0 M_c / 2\mu_0 H_0$.

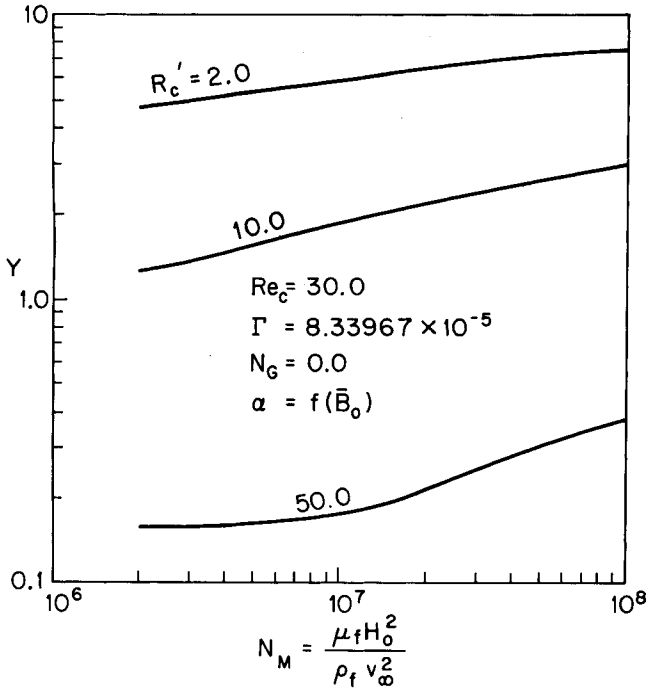

Fig. 14. Effect of particle size on capture cross section. The fluid is water, the collector is annealed iron, and the particle is copper oxide.

material and R_c are fixed, then Re_c and N_M are related through v_∞. For this case, the results are given in Figures 13, 14, and 15.

DISCUSSION OF RESULTS

The solutions developed in this work predict the capture of small ($< 10 \times 10^{-6}$ m) weakly paramagnetic particles by a single bare collector immersed in a magnetic field. A number of key assumptions have been made:

1. The collector is bare. The loading of the wire will change the shape of the collector and decrease the capture efficiency. Computational studies of the loading phenomena are now underway for both cylindrical and elliptical wires.

2. The collector is cylindrical. Many industrial collectors use a wire with a diamond shaped cross section. The magnetic field around the diamond shaped wire may enhance collection.

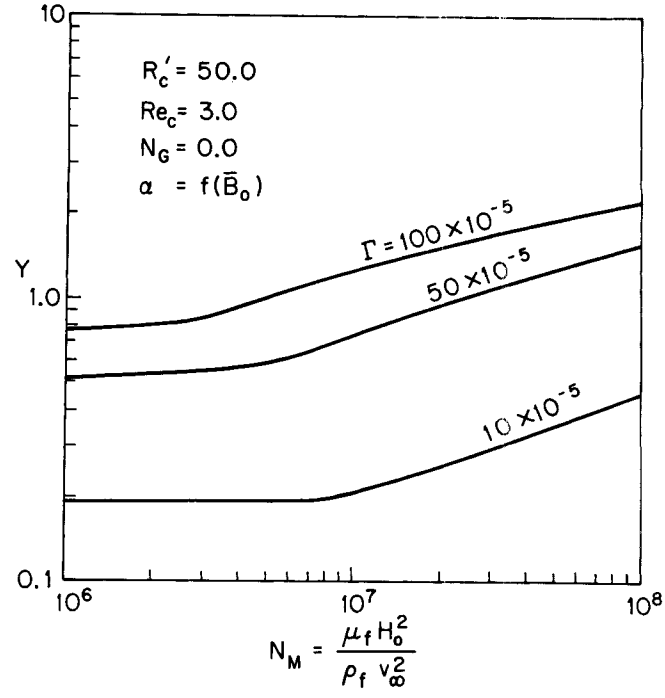

Fig. 15. Effect of particle permeability on capture cross section. The fluid is water and the collector material is annealed iron.

3. The particles are small compared to the collector. Some industrial separators use collectors with the same diameter as the particles. The assumptions used to compute the force on the particle in Equation (4) are not valid when the particle is of the same size as the collector. (In this case one needs to integrate the gradient throughout the volume of the particle.)

4. The particles are dilute. Some industrial separations are performed on concentrated suspensions. In addition, the suspension may contain both paramagnetic and diamagnetic particles with a wide particle size range.

5. The particles are homogeneous. It is possible to have a single particle which contains regions of different magnetic susceptibility. The computation of the force acting on these types of particles is more difficult than that given in Equation (4).

6. The collector is in homogeneous magnetic and flow fields. In a commercial separator the collector is surrounded by other collectors. Both the magnetic and flow fields surrounding these collectors interact to cause inhomogeneities.

7. The fluid is in potential flow around the collector. The absence of the no-slip boundary condition with potential flow may decrease the capture efficiency. The fluid velocity near the surface is lower with the no-slip condition.

8. The particle does not disturb the flow field around the collector. This will certainly not be the case when the particles are of the same size as the collector. In addition, the squeezing out of fluid between the particle and the collector will decrease the capture efficiency.

Even with these assumptions, a number of important features of the capture process can be observed. First, the magnetic forces are long range and partially justify assumptions 2, 6, 7, and 8. This is most evident in Figures 7 and 9. Second, the drag forces are important and dominate the capture process at small particle sizes. This is because the magnetic forces decrease as R_p^3 while the drag forces decrease as R_p^2. Third, all of those conditions

which promote particle capture (for example, increased field strength, increased particle permeability) tend towards a limit. This can be seen in Figures 10, 11, and 12. Fourth, many materials which are not ordinarily considered magnetic can be affected by fields in a high gradient separator. For aluminum, $\Gamma = 0.99 \times 10^{-5}$, for titanium, $\Gamma = 6.3 \times 10^{-5}$, for copper oxide, $\Gamma = 8.3 \times 10^{-5}$, for chromium, $\Gamma = 10.7 \times 10^{-5}$. All of these values lie within the range shown in Figure 12. From this analysis it is clear that a number of other features of the capture of paramagnetic particles remains to be studied, primarily the details of particle motion very near the collector. In a subsequent paper we examine the effects of London forces, fluid squeeze out, and the no-slip fluid flow boundary condition.

ACKNOWLEDGMENT

Part of this work was performed while the authors were in the Department of Chemical Engineering at the Massachusetts Institute of Technology, Cambridge, Massachusetts. Valuable suggestions were made by Dr. Dennis C. Prieve of the Department of Chemical Engineering, Carnegie-Mellon University.

NOTATION

$\mathbf{B}$ = magnetic field
$\mathbf{F}$ = force
$\mathbf{g}$ = gravitational acceleration constant
$\mathbf{H}$ = magnetic intensity
$\mathbf{i}$ = unit vector
$\mathbf{M}_{(s)}$ = magnetization (saturation)
N_g = dimensionless gravity group
N_M = magnetic intensity group
r = distance from origin
R = body radius
Re = Reynolds' number
$\mathbf{v}$ = velocity
V = volume
W = field energy

Greek Letters

α = dimensionless cylinder permeability
η = viscosity
μ = magnetic permeability
ρ = density
θ = angle referred to x axis (Figure 1)
Γ, γ = dimensionless particle permeability

Subscripts

c = cylinder
D = drag
f = fluid
g = gravity
M = magnetic
o = base value
p = particle
r = relative
x, y, r, θ = direction
S = sphere

Superscripts

$'$ = dimensionless
x, y, r, θ = direction

LITERATURE CITED

Bean, C. P., "Magnetic Filtration," *Am. Phys. Soc.*, **16**, 350 (1971).

DeLatour, C., "Magnetic Separation in Water Pollution Control," *IEEE Trans. Magnetics*, **Mag-9**, No. 3, 314 (1973).

Himmelblau, D. A., M.S. thesis, Department of Chemical Engineering, Mass. Inst. Technol., Cambridge (1974).

Kelland, D. R., "High Gradient Magnetic Separation Applied to Mineral Beneficiation," *IEEE Trans. Magnetics*, **Mag-9**, 307-310 (1973).

———, "Magnetic Separation of Non-magnetic Taconite," *Proceedings 35th Annual Mining Symposium*, Duluth, Minn. (1974).

Kolm, H., J. Oberteuffer, and D. Kelland, "High-Gradient Magnetic Separation," *Sci. Am.*, **233**, 46 (1975).

Lawver, J. E., and D. M. Hopstock, "Wet Magnetic Separation of Weakly Magnetic Materials—A State of the Art Review," *Minerals Sci. Eng.*, **6**, No. 3, 154 (1974).

Mamula, M., et al., "A Method of Separating Solid Substances Dispersed in a Liquid," *Czechoslovakian Patent #132624*, (June, 1969).

Oberteuffer, J. A., "High Gradient Magnetic Separation," *IEEE Trans. Magnetics*, **Mag-10**, No. 2, 223 (1974).

Stratton, J. A., *Electromagnetic Theory*, McGraw-Hill, New York (1941).

Trindade, S. C., H. H. Kolm, J. Howard, and G. J. Powers, "Magnetic Desulfurization of Coal," *Fuel*, **3**, 371 (1974).

Watson, J. H. P., "Magnetic Filtration," *J. Appl. Phys.*, **44**, No. 9, 4209 (1973).

———, "Magnetic Filtration," *IEEE Trans. Magnetics*, **Mag-11**, 1588 (1975).

Zebel, G., "The Capture of Particles in Electric Fields," *J. Colloid Sci.*, **20**, 522 (1965).

APPENDIX A: CONVERSION OF UNITS

Many literature sources describe the magnetic properties of materials by X_m, the magnetic susceptibility, in cgs units. Therefore, it is necessary to convert this data to units compatible with the SI.

$$\mu_o = 4\pi \times 10^{-7}\ h/m = \text{magnetic permeability of free space}$$

$$X_m = \left(\frac{\mu}{\mu_o} - 1\right) = \text{dimensionless magnetic susceptibility}$$

$$X_m\,(\text{mass}) = \left(\frac{\text{m}^3}{\text{kg}}\right) = \text{magnetic susceptibility/unit mass}$$

$$X_m\,(\text{molar}) = \left(\frac{\text{mole-m}^3}{\text{kg}}\right) = \text{magnetic susceptibility/mol. wgt.}$$

$$X_m = [X_m\,(\text{mass})]\,(\rho)$$

$$X_m = [X_m\,(\text{molar})]\,(\rho/\text{mol. wgt.})$$

$$X_m\,(\text{SI}) = 4\pi\,[X_m\,(\text{cgs})]$$

$$X_m\,(\text{mass, SI}) = 4\pi \times 10^{-3}\,[X_m\,(\text{mass, cgs})]$$

$$K_m = \left(\frac{\mu}{\mu_o}\right) = (1 + X_m) \equiv \text{relative permeability (another frequently listed property value)}$$

As an example, the particle considered in this work is copper oxide. The CRC Handbook of Physics and Chemistry reports:

$$X_m\,(\text{molar, cgs}) = 239 \times 10^{-6}$$

$$X_m\,(\text{cgs}) = 239 \times 10^{-6}\left(\frac{6.4}{79.54}\right) = 1.923 \times 10^{-5}$$

$$X_m\,(\text{SI}) = 4\pi\,(1.923 \times 10^{-5}) = 2.416 \times 10^{-4}$$

Manuscript received August 12, 1975; revision received and accepted March 10, 1976.